JOURNAL OF CATALYSIS 53, 68–87 (1978)

Reactions Involving Electron Transfer at Semiconducting Surfaces

VII. Interactions of Aliphatic Alcohols and Nitrous Oxide, on Reduced ZnO and TiO_2 Surfaces

JOSEPH CUNNINGHAM, DENIS J. MORRISSEY, AND EDWARD L. GOOLD

Chemistry Department, University College, Cork, Ireland

Received November 19, 1976; revised November 7, 1977

The simultaneous admission of nitrous oxide and the vapor of a primary or secondary alcohol at room temperature to ZnO or TiO_2 (rutile) samples, whose surfaces were prereduced by thermally outgassing *in vacuo* for 16 hr at 673 K, produced a doubling or trebling of the yield of nitrogen product relative to that observed with N_2O alone. The effect is attributed to dissociative electron attachment to N_2O, yielding O^- intermediates at the interface which then abstracted an α-hydrogen from primary or secondary alcohol and produced a second surface intermediate capable of reacting with other N_2O molecules. This sequence of events did not occur with tertiary alcohol at the nonilluminated metal oxide surfaces but 2-methyl-propan-2-ol was observed to undergo continuing photocatalyzed dehydration at ZnO or TiO_2 surfaces excited by photons of $\lambda = 340 \rightarrow 640$ nm. Continuing photodehydration was not observed with primary or secondary alcohols and the difference is explained in part by the greater stability of the cation formed from the tertiary alcohol through localization of a photogenerated hole and in part by the availability of another channel for photooxidation of the primary and secondary alcohols, viz. dehydrogenation. Photodehydrogenated products were observed from primary and secondary alcohols but in limited yields which were comparable to attainable levels of alcohol adsorption. The limitation on the extent of photodehydrogenation in the absence of an oxidizing gas would be understood on the basis that each surface O^- site was rendered inactive following one hole-capture-plus-dehydrogenation event.

INTRODUCTION

Earlier papers in this series considered one-electron transfer from semiconducting ZnO or TiO_2 to adsorbed N_2O molecules, both in terms of *indirect* electron transfer based on collective-electron Band Theory models and in terms of *direct* electron transfer from isolated electron-donating active sites on the ZnO or TiO_2 surfaces (*1–4*).

The present study explores the possibilities of utilizing adsorbed aliphatic alcohols as surface probes in analagous fashion to N_2O, but for the detection of electronic holes at ZnO or TiO_2 surfaces. Other workers have claimed that primary and secondary alcohols can be reactive toward electronic holes at ZnO surfaces, either via valence band interaction (*5*, *6*) or after hole capture by surface hydroxyls (*7–9*), and such processes would respectively be equivalent to *indirect* and *direct* hole transfer. The experimental conditions selected to examine the possibility of such *direct or indirect* hole transfers at ZnO or TiO_2 surfaces in the present study involved photogeneration of electronic holes by uv illunimation of *alcohol/metal oxide* interfaces. Since these metal oxides each

0021-9517/78/0531-0068$02.00/0

exhibit n-type semiconductivity and band gaps of ca. 3.1 eV (*10–11*), illumination by photons of energies greater than the band gap (e.g., photons of $\lambda > 300$ nm with energies <4.1 eV or photons of $\lambda = 254$ nm with energies 4.9 eV) should serve to produce photostationary hole concentrations, p^*, much greater than the very low hole concentrations, p, which would exist in these materials at room temperature in conditions of thermal equilibrium.

Direct or indirect interaction of adsorbed alcohol with electronic holes at uv-illuminated surfaces of ZnO or TiO_2 should yield oxidized products, such as corresponding ketones or aldehydes from selective photooxidation. The heterogeneously catalyzed photodehydrogenation of alcohols has been reported by many workers in the presence of molecular oxygen as oxidant (*7–9, 12, 13*). Photodehydrogenation of propan-2-ol to acetone has been particularly widely studied and various workers have interpreted their results in terms of direct hole transfer involving initially the capture of photogenerated holes by surface hydroxyls while adsorbed molecular oxygen acts as the electron trap (*7, 9*). This type of photocatalyzed "redox" process on the metal oxide catalyst should also be possible between alcohols and other electron-attaching molecules, such as N_2O, adsorbed on the metal oxide surface. The present study therefore also examines the advantages and disadvantages of utilizing N_2O as an alternative oxidant for photocatalyzed oxidation of alcohols on ZnO and TiO_2 at room temperature. Possible advantages include the well-established reactivity of N_2O toward one-electron reduction (*1, 4, 14*) and the lack of significant reactivity toward OH-radicals (*15*), plus the probability that dissociative electron attachment via Reaction (1)

$$N_2O_{(ads)} \xrightarrow{e^-} N_2O_{(ads)}^- \rightarrow N_{2(g)} + O_{(ads)}^- \qquad (1)$$

produces O^- as a well-defined oxygen intermediate (*16*) with selective reactivity toward primary and secondary alcohols (*17–19*). Thus Warman (*17, 18*) postulated that when N_2O was used as a source of O^- species in homogeneous gas-phase mixtures of (N_2O + alcohol) under irradiation, reactions (2a) and (2b) occur as secondary reactions in the presence of primary and secondary aliphatic alcohols but not with tertiary alcohol.

$$O^- + ROH \rightarrow (X + Y)^- \qquad (2a)$$

$$(X + Y)^- + mN_2O \rightarrow mN_2 + (\text{products}). \qquad (2b)$$

According to this scheme, the occurrence of O^- as an intermediate in appropriate (N_2O + alcohol) mixtures should yield added dissociation of N_2O to N_2. Although Warman did not positively identify the ionic intermediate, $(X + Y)^-$, subsequent studies on homogeneous liquid systems by pulse radiolysis techniques have demonstrated that selective abstraction of the hydrogen atom in the α-position relative to the alcoholic $-OH$ group is the dominant reaction pathway of O^- toward primary and secondary alcohols (*19*).

The foregoing paragraphs emphasize the roles of intermediates and reactions initiated by one-electron-transfer processes in alcohol systems under irradiation and their possible importance for photocatalyzed oxidation of (N_2O + alcohol) mixtures over metal oxide surfaces. The occurrence of one-electron-transfer processes involving molecules adsorbed on surfaces of ZnO and TiO_2 is supported by published results of ESR (*20–24*) and related studies (*4*). However, it is important to keep in mind that, in the absence of irradiation, metal oxide surfaces are also widely reported to exhibit Brønsted or Lewis acid–base characteristics in their interaction with alcohols or related organic molecules (*25–27*). Consequently, acid–base type interactions with the surface may also

be important, e.g., in determining the nature and extent of alcohol adsorption. Since it appeared from previous studies that prolonged outgassing of ZnO *in vacuo* at 623–673 K sufficed to reduce residual hydroxyls and any Brønsted activity to low levels (*3*, *4*, *28*), this pretreatment was adopted as standard for all the samples used in the present study, with a view to characterizing photocatalyzed reaction on "initially dehydroxylated" surfaces. An important role of Lewis acid–base-type interactions at appropriate surface sites, such as coordinatively unsaturated (*cus*) metal-ion or oxygen-ion sites, can be expected between alcohol and dehydroxylated surfaces in the absence of irradiation. Results of the present study will indicate, however, that one-electron localization/delocalization effects produced at the interfaces by uv illumination can indirectly influence the effective Lewis acid–base character of the metal oxide surfaces and hence modify their activity for alcohol dehydration.

EXPERIMENTAL

Materials

Powdered, high-purity metal oxides were identical to the ZnO (SP500) and TiO_2 (Rutile MR-128) used in previous studies and were obtained by courtesy of New Jersey Zinc Co. Thin polycrystalline layers on quartz tubing were prepared and dehydroxylated *in vacuo* at 673 K, as previously described (*4*). Analar reagent grade alcohols were dried over freshly dehydrated molecular sieve and purified by trap-to-trap distillations, except for anhydrous C_2D_5OD or $(CD_3)_2CDOD$ which were used as supplied by Stohler Isotopes. High purity nitrous oxide, or oxygen (BOC Grade X), were used as obtained.

Adsorption

Since it was known from previous studies that ZnO or TiO_2 surfaces outgassed *in vacuo* for 16 hr at 673 K contained a limited number of reactive metal-excess surface centers, it was necessary in the present study to examine the initial interaction of the alcohol alone and of nitrous oxide alone with such reduced surfaces prior to examining surface interactions of premixed (alcohol + N_2O) mixtures. Extent of room temperature adsorption of individual components onto prereduced samples was measured with a vacuum microbalance (Sartorius Model No. 4102). Electron spin resonance spectrometers with capability for maintaining prereduced samples at 77 K (Decca X-1 or Varian T2 spectrometers) were utilized to observe effects of alcohol upon ESR spectra of paramagnetic metal excess centers on the ZnO or TiO_2 surfaces.

Gaseous Product Formation over Nonilluminated Samples

Observations on the gas phase above nonilluminated samples were made with the closed quartz reactor and associated greaseless high-vacuum system schematically depicted in Fig. 1A. Usually products were monitored only from room temperature interactions of alcohols and/or nitrous oxide with a metal oxide sample previously activated for 16 hr *in vacuo* at 673 K. Products noncondensable (n.c.) at 77 K were measured with Pirani or ionization gauges and identified with a CEC type 21-620A mass spectrometer during periodic freezing out of reactants into a trap at 77 K. Condensable products were monitored through mass spectral analysis of the condensable gases. Since such measurements could only monitor growth of those products which desorbed from the catalyst surface at room temperature, some catalyst samples, which had been exposed to alcohol and/or nitrous oxide at room temperature, were then heated *in vacuo* by 50 K increments to 673 K, during which time measurements

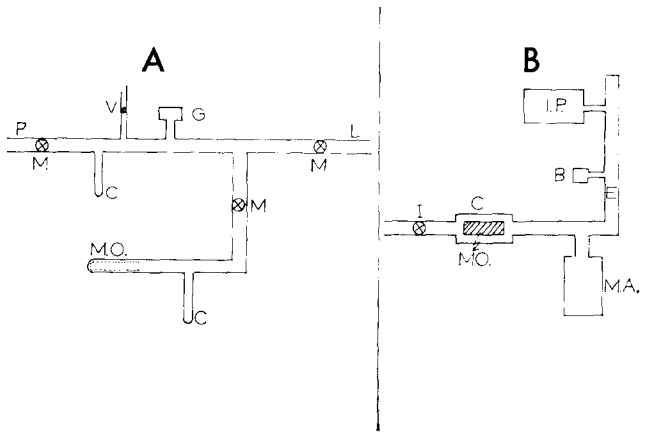

FIG. 1. Vacuum systems for study of gaseous products evolved from interfaces of ZnO and TiO_2 with N_2O and/or aliphatic alcohols: (A) Static reactor with: pumping line, P; gas handling line, L; Pirani gauge, G; variable leak valve, V; metal valves, M; cold fingers, C; and metal oxide sample, M.O. (B) Dynamic reactor with: inlet leak valve, I; metal oxide layer, M.O.; stainless-steel tubing, E; glass-walled photoreactor, C; Micromass 6 mass analyzer, M.A.; pressure gauge, B; and ion pump, I.P.

were made on the pressure and mass spectra of gases thermally desorbed over each 50 K increment.

Photoassisted Surface Reactions

Interfaces between metal oxide sample and alcohol or (alcohol + N_2O) mixtures, which had completed the fast "dark reaction" characteristic of initial 0.5-hr contact times with prereduced surfaces, were then exposed to continuous uv illumination at low intensity in order to observe any additional photoassisted reactions on the surface. Low wattage mercury-arc lamps were used for continuous uv illumination, viz. a Hanau 150-W medium-pressure burner fitted with a Pyrex water-cooled jacket when illumination at $\lambda > 300$ nm was desired or a Hanau 15-W low-pressure burner when photons mainly at 254 nm were required and gas phase pressure of reactants was sufficiently low to avoid significant gas phase absorption and photolysis. Lamp configuration within an MgO-coated cavity was such as to maximize the percentage of lamp output reflected onto the sample, but temperature rise at the samples was less than 10 K in all cases. Such temperature rises, when induced thermally, did not significantly disturb the equilibria reached in the absence of uv illumination. Growth of any product which desorbed into the gas phase at room temperature under continuous illumination was followed and analyzed over periods of illumination up to 6 hr in the same system as employed for dark reaction. Photon flux at the sample position was determined by calibration with potassium ferrioxalate actionometer. Results obtained at uv illuminated interfaces are indicated by use of an asterisk, e.g. $(CH_3)_2CHOH/TiO_2$*. Release of photoproducts from such interfaces at very low pressures, ca. 10^{-4} N m^{-2}, was studied with the dynamic flow photoreactor shown in Fig. 1B.

RESULTS: SECTION A—INTERACTIONS ON NONILLUMINATED SURFACES

A.1. Adsorption

Table 1 summarizes adsorption data derived from weight increases measured with the vacuum microbalance for 300-mg

TABLE 1

Pseudoequilibrium Values for Room Temperature Adsorption on Prereduced ZnO and TiO_2 (Expressed as Molecules per m^2 of Oxide Surface at Indicated Pressures)

Metal-oxide/gas	Pressure				Type of adsorption
	0.26 N m^{-2}	13 N m^{-2}	133 N m^{-2}	10^3 N m^{-2}	
$ZnO/(CH_3)_2CHOH$	—	2×10^{18}	2.3×10^{18}	2.6×10^{18}	Total
$ZnO/(CH_3)_2CHOH$	—	2×10^{17}	3.1×10^{17}	3.8×10^{17}	Reversible
$TiO_2/(CH_3)_2CHOH$	—	1.7×10^{18}	2.1×10^{18}	—	Total
$TiO_2/(CH_3)_2CHOH$	—	3.8×10^{17}	4.6×10^{17}	—	Reversible
$ZnO/(CH_3)_3COH$	—	1.6×10^{18}	2.1×10^{18}	2.4×10^{18}	Total
$ZnO/(CH_3)_3COH$	—	1.7×10^{17}	2×10^{17}	3.6×10^{17}	Reversible
$TiO_2/(CH_3)_3COH$	—	2.2×10^{18}	2.9×10^{18}	2.4×10^{18}	Total
$TiO_2/(CH_3)_3COH$	—	2.8×10^{17}	5.6×10^{18}	10^{18}	Reversible
ZnO/CH_3CH_2OH	2.6×10^{16}	1.3×10^{17}	—	—	Total
ZnO/CH_3CH_2OH	2.6×10^{16}	1.3×10^{17}	—	—	Reversible
TiO_2/CH_3CH_2OH	3.9×10^{17}	5.0×10^{17}	6.7×10^{17}	—	Total
TiO_3/CH_3CH_2OH	3.3×10^{17}	3.8×10^{17}	—	—	Reversible
TiO_2/N_2O	—	—	3.6×10^{17}	1.1×10^{18}	Total
TiO_2/N_2O	—	—	1.6×10^{17}	6.5×10^{17}	Reversible

samples of prereduced ZnO or TiO_2 after 1800-sec exposure to constant equilibrium vapor pressure of the indicated alcohol. Constant pressures were maintained by immersing reservoirs of the purified and outgassed alcohols in appropriate refrigerated constant-temperature baths. Values in Table 1 are pseudoequilibrium, rather than true equilibrium, values since sample weight continued to increase for many hours during exposure in these conditions, albeit at a very slow rate. However, weight increases at 1800 sec represented $>80\%$ of those at longer times and so provided a good approximation to the total amount of alcohol-related species adsorbed at room temperature at the alcohol pressures indicated in Table 1. Pseudoequilibrium values for total extent of adsorption of the various alcohols at room temperature onto ZnO or TiO_2 were adequately represented over the pressure range, 1 to 10^3 N m^{-2}, by Freundlich-isotherm-type plots. Comparison of the values for total adsorption of the various alcohols reveals that the secondary and tertiary alcohols adsorbed to comparable extent, which corresponded to ca. 0.5 ± 0.2 of monolayer coverage, but that total adsorption of ethanol was appreciably lower.

Table 1 also shows the amount of initially adsorbed alcohol which was removed by reevacuation to 10^{-3} N m^{-2} at room temperature. Those values are denoted in Table 1 as "reversibly" adsorbed, and it is notable that such reversibly adsorbed alcohol represented a much larger percentage of the adsorbed total for ethanol than for isopropanol or 2-methyl-propan-2-ol. For these latter cases the predominant component of alcohol-related species on the prereduced ZnO and TiO_2 surfaces could be classed as "irreversibly adsorbed" at room temperature, since it was not removed by prolonged evacuation at 300 K but required heating to ca. 670 K for its complete removal. This ability of the irreversibly adsorbed alcohol species to withstand prolonged outgassing at 300 K showed that no significant conversion occurred to reversibly adsorbed species at room temperature. Predominance of the irreversibly adsorbed species on the surfaces

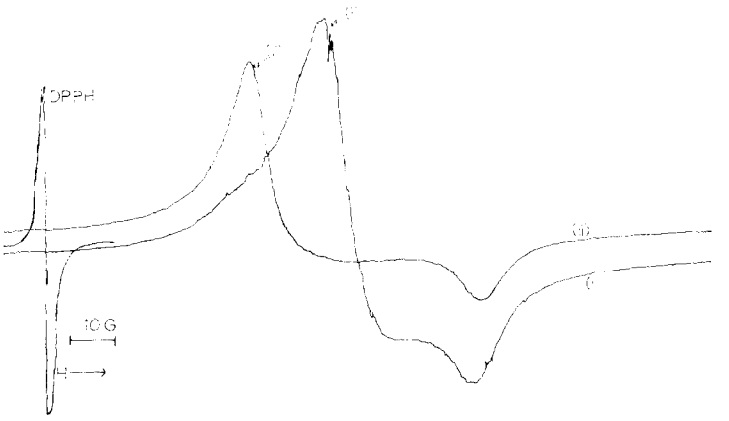

FIG. 2. Electron spin resonance spectra of powdered TiO_2 (rutile) sample taken at 77 K: (i) Sample *in vacuo* after outgassing at 673 K; (ii) after exposure for 600 sec at 293 K to vapor of C_2H_5OH followed by evacuation at that temperature.

of ZnO and TiO_2 following their exposure to $(CH_3)_2CHOH$ or $(CH_3)_3COH$ should strongly favor surface reactions involving those species rather than reversibly adsorbed alcohol. It may also be concluded, from the observed slow approach toward adsorption equilibrium in these systems (e.g., $t_{\frac{1}{2}} > 300$ sec), that appreciable fractions of adsorption sites remained uncovered by alcohol species up to such exposure times.

Pseudoequilibrium values were also measured for adsorption of nitrous oxide onto prereduced ZnO and TiO_2 and results are entered in Table 1. These show smaller extent of coverage by adsorbed species derived from N_2O than was the case for adsorbed species derived from secondary or tertiary alcohol at 133 N m^{-2} but show comparable total adsorption of N_2O to that for ethanol at this pressure.

A.2. ESR

The ESR spectra shown in Fig. 2 for powdered rutile samples provide evidence that primary or secondary alcohol species irreversibly adsorbed onto prereduced TiO_2 did not affect the degree of localization/delocalization of unpaired electrons at the rutile surface. Thus spectrum (i), which was measured at 77 K on an evacuated TiO_2 sample prereduced at 673 K, corresponds well to the broad anisotropic resonance usually attributed to paramagnetic Ti^{3+} centers at the TiO_2 surface. Spectrum (i) was not significantly altered if the sample was warmed *in vacuo* to 300 K and again cooled to 77 K, but a new spectrum (ii) resulted if such samples were exposed to the saturation vapor pressure of ethanol or butan-2-ol for 600 sec and reevacuated for 1800 sec before recooling to 77 K. The differences between spectra (i) and (ii) are small but unmistakable and were repeated with several samples. Furthermore, they could be reversed by heating the alcohol-exposed sample to 673 K under evacuation. These small but reproducible changes in shape of the Ti^{3+} resonance brought about by alcohol species irreversibly adsorbed on the surface at room temperature correspond to a slight increase in $g_\perp$ from 1.968 to 1.977. This indicated only a weak dipolar interaction between irreversibly chemisorbed alcohol and the unpaired electron of Ti^{3+}, such as could arise by changes in degree of coordinative unsaturation of Ti^{3+} through dative bonding via a lone pair of electrons on the alcohol–OH group. The absence of any marked change

TABLE 2

Extent and Rate of Formation of N_2 Product upon Simultaneously Contacting (Alcohol + N_2O) with Prereduced Surfaces of ZnO or TiO_2 at Room Temperature without uv Illumination

System	P_0 (React) (/N m^{-2})	$V(N_2)_{lim}$ (/molecules m^{-2})	k_d (/sec^{-1})
A. Zinc oxide surfaces prereduced for 16 hr at 623 K			
$\{N_2O + C_2H_5OH\}/ZnO$	45 (each)	2.1×10^{15}	1.5×10^{-3}
$\{N_2O + (CH_3)_2CHOH\}/ZnO$	45 (each)	2.1×10^{15}	1.4×10^{-3}
$\{N_2O + (CH_3)_3COH\}/ZnO$	45 (each)	9.5×10^{14}	2.8×10^{-3}
N_2O/ZnO	45	1.1×10^{15}	1.4×10^{-3}
B. TiO_2 (rutile) surfaces prereduced for 16 hr at 623 K			
$\{N_2O + C_2H_5OH\}/TiO_2$	45 (each)	1.9×10^{16}	2.3×10^{-3}
$\{N_2O + (CH_3)_2CHOH\}/TiO_2$	45 (each)	1.9×10^{16}	2.5×10^{-3}
$\{N_2O + (CH_3)_3COH\}/TiO_2$	45 (each)	5.4×10^{15}	2.1×10^{-3}
N_2O/TiO_2	45	6.3×10^{15}	1.0×10^{-3}

in integrated intensity between spectra (i) and (ii) would not be consistent with appreciable one-electron charge transfer between alcohol and the prereduced TiO_2 surface, since a decrease in ESR signal intensity due to Ti^{3+} would be expected if one-electron transfer occurred between chemisorbed alcohol and Ti^{3+} to yield surface carbonium or carbanion ion radicals.

A.3. Nitrogen Product from N_2O/ZnO and (N_2O + Alcohol)/ZnO Interfaces at Room Temperature

The extent of formation of nitrogen product was strongly influenced by the sequence in which nitrous oxide and alcohol were admitted. Thus Fig. 3A (i) illustrates the rapid growth of gaseous product noncondensable at 77 K to a limiting value, $V(N_2)_{lim}$, which occurred during the first hour of contact at room temperature between freshly activated ZnO and nitrous oxide. No such yield of nitrogen product was observed if alcohol was adsorbed prior to admitting nitrous oxide. Plots (ii) of Figs. 3A and B demonstrate, however, that the limiting yield of noncondensable product, $V(N_2)_{lim}$, as observed at room-temperature contact times >60 min, was greatly enhanced when either ethanol or isopropanol was premixed with N_2O in 1:1 mole ratio, so that alcohol and nitrous oxide simultaneously contacted the prereduced surface. Mass spectrometric analysis of the noncondensable product established that it was >98% nitrogen and that no nitric oxide or oxygen was detectable. Empirical kinetic analysis showed that the increase in nitrogen product, $V(N_2)_t$, detected after dark contact time t, obeyed the first-order type expression,

$$\log\left[\frac{V(N_2)_{lim}}{V(N_2)_{lim} - V(N_2)_t}\right] = k_d t, \quad (3)$$

for contact times 5–30 min, either for N_2O alone or for (N_2O + alcohol) mixtures. Table 2 summarizes the values of $V(N_2)_{lim}$ and k_d which gave the "best fit" of data to this expression. These data show (a) that nitrogen product formation from nitrous oxide at contact times >60 min, $V(N_2)_{lim}$, was approximately doubled by premixing ethanol or isopropanol with the nitrous oxide admitted to the freshly activated ZnO surface, and (b) that the apparently first-order rate constant, k_d, for dissociation of N_2O to N_2 at the "dark" ZnO surfaces was not significantly

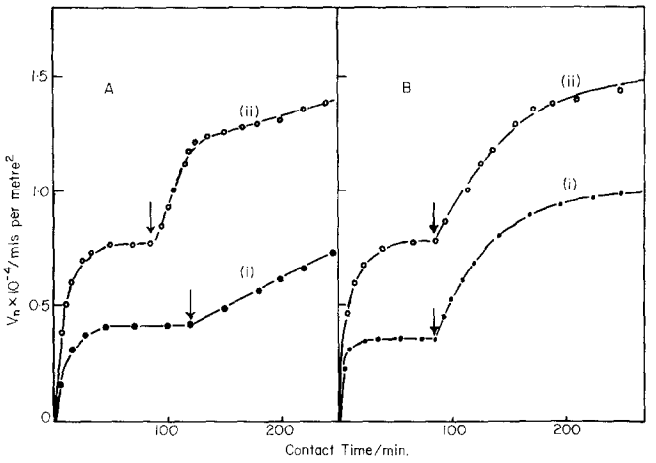

FIG. 3. Evolution of N_2 product from ZnO surfaces at 293 K (position of arrow denotes commencement of illumination): (Ai) N_2O/ZnO with $P\{N_2O\} = 45$ N m^{-2}; (Aii) $\{N_2O + C_2H_5OH\}$/ZnO with $P\{N_2O\} = 45$ N m^{-2}, $P\{C_2H_5OH\} = 45$ N m^{-2}; (Bi) $\{N_2O + (CH_3)_3COH)\}$/ZnO with $P\{N_2O\} = 45$ N m^{-2}, $P\{(CH_3)_3COH\} = 45$ N m^{-2}; (Bii) $\{N_2O + (CH_3)_2CHOH\}$/ZnO with $P\{N_2O\} = 45$ N m^{-2}, $P\{(CH_3)_2CHOH\} = 45$ N m^{-2}.

affected by premixed ethanol or isopropanol.

Effects noted with the tertiary alcohol, 2-methyl-propan-2-ol, premixed in equimolar ratio with N_2O prior to their simultaneous contact with the prereduced ZnO surface, were in marked contrast to (a) and (b) above, since $V(N_2)_{lim}$ was slightly reduced whereas k_d was increased (cf. Table 2). The effects of the various alcohols upon $V(N_2)_{lim}$ so closely paralleled those reported by Warman (see Introduction) that an analogous interpretation was suggested, viz. that initial dissociation of N_2O occurred via Reaction (1) on the metal oxide and that the resultant short-lived $O_{(ads)}^-$ species reacted rapidly with primary or secondary alcohol via Reaction (2a) producing surface intermediates, $(X+Y)^-$, which in turn rapidly dissociated other N_2O molecules via Reaction (2b). Our observation that admixed 2-methyl-propan-2-ol did not increase $V(N_2)_{lim}$ appeared consistent with Warman's conclusion that tertiary alcohols cannot react with O^- via type Reaction (2a). The different effects of alcohols upon k_d could be understood on the basis that the slow rate-determining step was contained in Reaction (1) [rather than in Reactions (2a) or (2b)] and was enhanced only by the greater electron-donating properties of the tertiary alcohol toward the ZnO surface. Another experimental result which favored particularly strong interaction of the tertiary alcohol with prereduced ZnO surfaces was the detection of alkene and alkane product (cf. A.5 below) upon initial contact, whereas no such product accompanied contact with ethanol or isopropanol.

A.4. Nitrogen Product from N_2O/TiO_2 and (N_2O + Alcohol)/TiO_2 Interfaces at Room Temperature

Qualitatively similar dependence of the extent of dissociation to nitrogen upon the sequence followed in admission of the nitrous oxide and alcohol was observed with TiO_2. Data to the left of the arrows in Fig. 4 illustrate growth of nitrogen product during the first hour of contact of freshly activated nonilluminated TiO_2 with N_2O alone or with a premixed (N_2O + alcohol) reactant gas. Empirical kinetic analysis again established that data for

contact times 5–30 min could be adequately fitted to the first-order type Eq. (3). Table 2B lists values so determined for $V(N_2)_{lim}$ and k_d over the TiO_2 surface. Inspection of the $V(N_2)_{lim}$ values reveals that at room temperature the tertiary alcohol, 2-methyl-propan-2-ol, failed to enhance nitrogen product formation at the dark N_2O/TiO_2 interface, whereas admixture of ethanol or isopropanol greatly enhanced $V(N_2)_{lim}$ relative to that with only N_2O present. Comparison of data in Table 2B with Table 2A reveals that admixtures of ethanol or isopropanol with N_2O trebled the limiting yield of nitrogen product $V(N_2)_{lim}$ observed when contacted with TiO_2, which exceeded the doubling produced upon contact with ZnO. Since enhancement by a factor of 3 was just that noted by Warman (*17, 18*) for reaction with gas phase O^-, present observations indicate that O^- intermediates on TiO_2 surfaces reacted with these alcohols with stoichiometry similar to that reported for Reactions (2a) and (2b) in the gas phase. The smaller enhancement of (N_2) noted in Table 2 for corresponding ZnO interfaces may then be attributed to loss of some fraction of surface O^- radicals into the ZnO bulk by hole migration, as inferred by Lunsford *et al.* for the N_2O/ZnO interface (*16*). The observed ability of admixed primary, secondary, or tertiary alcohol to approximately double k_d from nitrogen production over (N_2O + alcohol)/TiO_2 interfaces relative to that over the N_2O/TiO_2 interface also differed from corresponding results with ZnO, for which only the tertiary alcohol was effective. This difference may be understood in terms of the greater acidity of the TiO_2 surface (*26, 28*) which facilitated acid–base interactions with all the alcohols rather than with just the more basic tertiary alcohol, as occurred on ZnO.

A.5. Desorption from Alcohol/Metal-Oxide Interfaces

Careful monitoring of the gas phase over the various alcohol/metal-oxide interfaces at room temperature in a 1-hr period following contact of alcohol vapor with the prereduced ZnO or TiO_2 surface showed the absence of detectable gaseous products, except over the 2-methyl-propan-2-ol/TiO_2 interface which gave very small yields of 2-methyl-propene (1.6×10^{15} m^{-2}) and methane (0.8×10^{15} molecules m^{-2}). Data in Table 3 show that very much

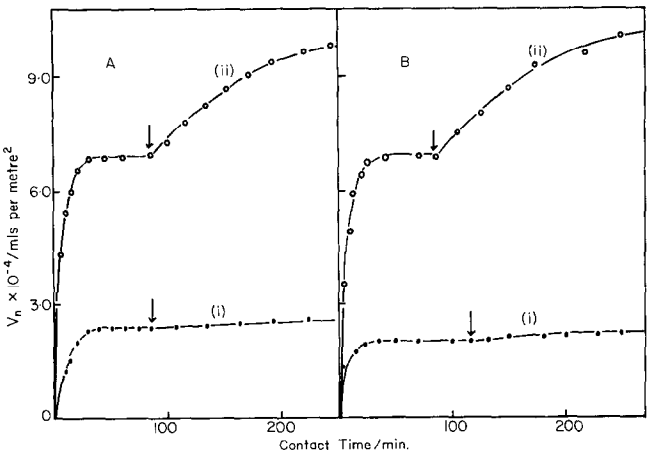

FIG. 4. Evolution of N_2 product from TiO_2 surfaces at 293 K: (Ai) N_2O/TiO_2; (Aii) {N_2O + C_2H_5OH}/TiO_2; (Bi) {N_2O + $(CH_3)_3COH$}/TiO_2; (Bii) {N_2O + $(CH_3)_2CHOH$}/TiO_2.

TABLE 3

Extent of Desorption of Various Products from Alcohol/Metal-Oxide Interfaces following Adsorption at Room Temperature onto Prereduced Surfaces

Alcohol/metal oxide	300 K		300–460 K		460–620 K	
Product	CH_4	$(-H_2O)$	$(-H_2O)$	$H_2(g)$	$(CH_3)_2CO$	"CH_3CHO"
$(CH_3)_3COH/ZnO$	—		4.3×10^{17}	—	—	
$(CH_3)_3COH/ZnO$*[a]	1.9×10^{15}	2.4×10^{15}	4.9×10^{17}	—	5.4×10^{14}	
$\{N_2O + (CH_3)_3COH\}/ZnO$	—		4.3×10^{17}	—	2.7×10^{14}	
$\{N_2O + (CH_3)_3COH\}/ZnO$*	2.4×10^{15}		4.6×10^{17}	—	3.2×10^{15}	
$(CH_3)_2CHOH/ZnO$	—	—	1.0×10^{17}	4.3×10^{17}	5.1×10^{16}	—
$(CH_3)_2CHOH/ZnO$*	—	—	1.0×10^{17}	3.0×10^{17}	5.9×10^{16}	—
$\{N_2O + (CH_3)_2CHOH\}/ZnO$	—	—	7.6×10^{16}	2.3×10^{17}	7.6×10^{16}	—
$\{N_2O + (CH_3)_2CHOH\}/ZnO$*	—	—	6.8×10^{16}	2.0×10^{17}	1.5×10^{17}	—
CH_3CH_2OH/ZnO	—	—	1.2×10^{17}	4.6×10^{17}		3.8×10^{16}[b]
CH_3CH_2OH/ZnO*	—	—	1.4×10^{17}	4.9×10^{17}		5.1×10^{16}
$\{N_2O + CH_3CH_2OH\}/ZnO$	—	—	8.6×10^{16}	3.8×10^{17}		7.2×10^{16}
$\{N_2O + CH_3CH_2OH\}/ZnO$*	—	—	1.2×10^{17}	4.1×10^{17}		7.3×10^{16}
$(CH_3)_3COH/TiO_2$	0.8×10^{15}	1.6×10^{15}	2.2×10^{18}[c]	—	—	—
$(CH_3)_3COH/TiO_2$*	2.7×10^{15}	1.1×10^{17}	2.7×10^{18}	—	4.1×10^{16}	—
$\{N_2O + (CH_3)_3COH\}/TiO_2$	—	—	1.9×10^{18}	—	—	—
$\{N_2O + (CH_3)_3COH\}/TiO_2$	4.1×10^{15}	4.6×10^{16}	2.7×10^{18}	—	9.2×10^{16}	—
$(CH_3)_2CHOH/TiO_2$	—	—	1.9×10^{18}[c]	—	—	1.8×10^{17}[b]
$(CH_3)_2CHOH/TiO_2$*	—	—	1.6×10^{18}	—	1.3×10^{16}	3.8×10^{17}
$\{N_2O + (CH_3)_2CHOH\}/TiO_2$	—	—	1.3×10^{18}	—	5.4×10^{15}	1.2×10^{17}
$\{N_2O + (CH_3)_2CHOH\}/TiO_2$*	—	—	1.2×10^{18}	—	4.3	2.7×10^{17}
$(CH_3CH_2OH/TiO_2$	—	—	5.1×10^{17}[c]	1.6×10^{16}	—	3.5×10^{17}[b]
CH_3CH_2OH/TiO_2*	—	—	5.1×10^{17}	5.7×10^{16}	—	1.1×10^{17}
$\{N_2O + CH_3CH_2OH\}/TiO_2$	—	—	1.6×10^{17}	5.4×10^{15}	—	8.1×10^{17}
$\{N_2O + CH_3CH_2OH\}/TiO_2$*	—	—	2.6	—	—	3.2×10^{17}

[a] Asterisk (*) indicates that the interface was exposed to uv illumination for 5×10^3 sec prior to heating.
[b] Detected as acetaldehyde decomposition products (butadiene + CO_2 + methyl acetylene + propene).
[c] Alkene product desorbed from TiO_2 over a slightly wider temperature range, 300–510 K, than from ZnO.

larger yields of various products were released to the gas phase during thermally assisted desorption from the alcohol/metal-oxide interfaces after gas phase and any reversibly adsorbed alcohol was pumped away at 300 K. Similar experiments were previously reported by Bickley and Jayanty (*8*) using a temperature-programmed desorption technique and present results agree with theirs in showing dehydrogenated and dehydrated products as the major components of desorbed gases.

Significant numbers of "active sites" capable of alcohol dehydration are indicated by thermal desorption of corresponding alkene in readily measurable amount (tabled under $-H_2O$ in Table 3). This was true for both ZnO and TiO_2, but the specific activity of TiO_2 was greater in all cases. For the TiO_2 surface, extent-of-alcohol dehydration increased in the sequence tertiary > secondary > primary, which is the same as that usually observed for alcohol dehydration by acid-type centers in homogeneous or heterogeneous catalysis (*30, 31*). Appearance of the olefine product at temperatures much below those previously reported (*32*) indicates that some, at least, of the dehydration sites on prereduced ZnO and TiO were of unusually high activity.

As expected, no dehydrogenated product was obtained from the tertiary alcohol but the ratio (dehydrogenation/dehydration) increased for isopropanol and ethanol. Thermally assisted desorption of the anticipated dehydrogenation products occurred to lesser extent than release of dehydrated products or of molecular hydrogen at temperatures <498 K. The histograms in

Fig. 5 illustrate the higher desorption temperatures required for release of acetone product than for propene or hydrogen desorption from the *isopropanol/ZnO* interface. The acetone histogram also represents (by the fully blackened sections) the thermal desorption behavior noted for the same surface when acetone rather than alcohol was initially absorbed at room temperature. At the higher temperatures required for desorption of aldehydes or ketones, thermally assisted rearrangements occurred, as evidenced by partial conversion of preadsorbed acetone to isobutene or of preadsorbed acetaldehyde to 1,3-butadiene. Extent of ethanol dissociation corresponding to products related to adsorbed acetaldehyde is tabled under (CH_3CHO) in Table 3. This latter observation contrasts with a report by McArthur *et al.* (*33*) that acetaldehyde desorbed readily from ZnO and the difference suggests that ethanol selectively displaced acetaldehyde at the temperatures employed in that study.

It must be emphasized here that the data summarized in Table 3 cannot provide reliable absolute values for surface densities of sites active for alcohol dehydration or dehydrogenation *at room temperature*, because of the probability of thermally activating additional sites during the desorption procedure. They can, however, provide "baseline" values for comparison with amounts of product thermally desorbed from the same interfaces in different conditions, e.g., when exposed to nitrous oxide admixed with the alcohol (see below) or to uv illumination (see Section B).

Admixture of nitrous oxide with the ethanol admitted to dark ZnO or TiO_2 caused a definite increase in products attributable to acetaldehyde (which then suffered further degradation upon thermal desorption). This observation, and a smaller increase in acetone from isopropanol, appeared consistent with the working hypothesis developed above in Section A.3, according to which nitrous oxide dissociates

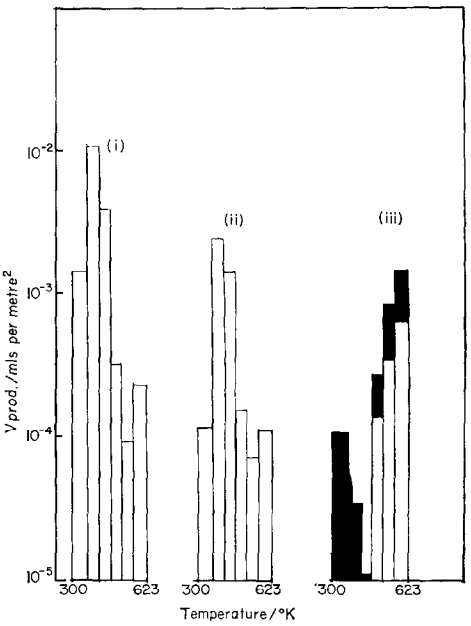

FIG. 5. Histograms for thermal desorption of various products from $(CH_3)_2CHOH/ZnO$ interfaces on heating to 673 K. (i) H_2 evolution; (ii) propene; (iii) acetone [darkened sections represent thermal desorption of $(CH_3)_2CO$ from a $(CH_3)_2CO/ZnO$ interface].

on the surfaces to yield O^- fragments which enhance dehydrogenation by then abstracting α-hydrogen from primary or secondary alcohol. Data in Table 3 show that dehydration products experienced a decrease when N_2O was admixed with primary or secondary alcohols, in contrast to the increases which N_2O brought about in dehydrogenation.

SECTION B—INTERACTIONS ON uv-ILLUMINATED SURFACES

B.1. N_2O/ZnO^* or TiO_2^*

A marked difference between these interfaces was that when uv illumination became incident, following dark equilibration of the interfaces as described in Section A, an appreciable enhancement in yield of nitrogen product was detected for N_2O/ZnO^* but not for N_2O/TiO_2^*. This difference can be seen by comparison of

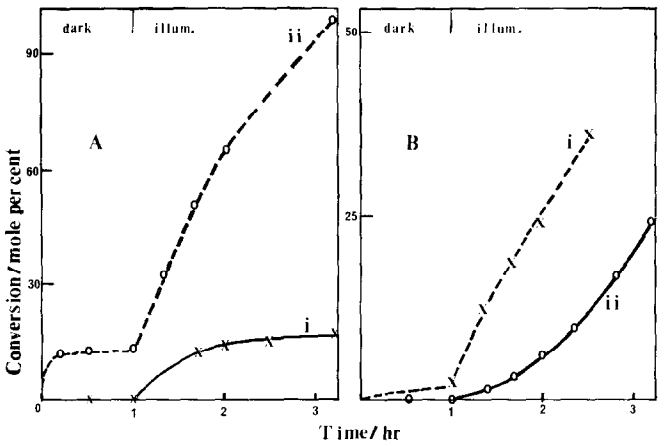

FIG. 6. Growth of gaseous photoproducts over $(CH_3)_3COH$/metal-oxide interfaces in a static photoreactor at room temperature under continuous illumination by photons of $\lambda > 300$ nm at alcohol pressures ca. 133 N m^{-2}. (A) Methane product over (i) prereduced ZnO; (ii) prereduced TiO_2. (B) Alkene product (2-methyl-propene) over (i) prereduced ZnO; (ii) prereduced TiO_2.

points to the right of the arrow on plots labled (1) on Figs. 3A and 4A, which were observed under illumination by photons mainly at 254 nm. Enhanced yield of nitrogen product was observed over N_2O/ZnO* interfaces under illumination by photons of $\lambda > 300$ nm. Studies at nitrous oxide pressures 10^2–5×10^4 N m^{-2} established that dependence of this photoassisted process upon pressure of nitrous oxide obeyed the Freundlich-type expression, log rate $= 1/n^{-1} \log P_{N_2O}$ + constant, where $n = 3.5$. Dependence of photoassisted rate upon θ_{N_2O}, the surface coverage by N_2O, allied to a Freundlich-type isotherm, $\theta_{N_2O} = C \cdot P^{1/n}$, for N_2O absorption upon ZnO, would explain the relation of rate to P_{N_2O}. A corollary of this explanation, however, would be that the rate and quantum efficiency of this photoassisted process must fall to very low values at low N_2O pressures, such as encountered in Section B.4.

B.2. Alcohols/ZnO or TiO_2**

The incidence of uv illumination onto these dark-equilibrated interfaces in the static photoreactor did not result in photoassisted release of additional product into the gas phase at room temperature, except with the tertiary alcohol, 2-methyl-propan-2-ol. Figure 6A illustrates the growth of methane photoproduct from this tertiary alcohol under illumination by photons of $\lambda > 300$ nm over ZnO. Methane product was also readily detected and followed to 100% conversion over TiO_2* surfaces but was accompanied by smaller conversion to 2-methyl-propene (cf. Figs. 6A and B). Increased amounts of this dehydration product were released from C_4H_9OH/ZnO* interfaces at room temperature as illustrated in Fig. 6B. Data in that figure establish clearly the occurrence of photoassisted dehydration at these *tertiary alcohol/metal-oxide* interfaces under illumination by photons of wavelengths >300 nm.

Since illumination of the alcohol/metal-oxide interfaces by photons of $\lambda > 300$ nm yielded only traces of dehydrogenated product in the gas phase at room temperature, thermal desorption studies similar to those detailed above for nonilluminated alcohol/metal-oxide interfaces were undertaken with the static reactor system in efforts to detect any products remaining

irreversibly adsorbed at room temperature after their formation by photodehydrogenation. Results of these studies are summarized in Table 3 and illustrate the difficulty of picking out photoassisted processes in cases where the thermal desorption process gave rise to a large background yield of the product under study. Despite this difficulty, data in Table 3 from the $(CH_3)_3COH/TiO_2$ system do provide support for a detectable increase in yield of 2-methylpropene and acetone under uv illumination, as already reported from these laboratories employing pulsed uv illumination and a fast response dynamic mass spectrometer technique (*34*). Data in Table 3 for the $\{N_2O+(CH_3)_2CHOH\}$ mixtures suggested that an enhanced yield of acetone occurred over ZnO and TiO_2 interfaces under continuous uv illumination. This possibility was further examined with the dynamic flow reactor arrangement illustrated in Fig. 1B (cf. Section B.4 below).

B.3. Photoassisted Processes in the Static Photoreactor over Metal Oxide Surfaces Contacted with (N_2O + Alcohol) Mixtures

Data points to the right of an arrow on each plot in Fig. 3 show that illumination by uv light mainly at 254 nm caused additional photoassisted dissociation to nitrogen product at ZnO interfaces which previously had attained their limiting value of $V(N_2)_{lim}$ in the dark. Two contributions to this photoassisted dissociation can be distinguished on the traces in Fig. 3: (a) an initially rapid photoassisted growth of nitrogen product which persisted only during the initial 1800 sec of uv illumination and was detected only in the presence of alcohol admixed with N_2O—this is well illustrated for the $\{N_2O + C_2H_5OH\}/ZnO^*$ interface on plot (ii) of Fig. 3A, and (b) a subsequent slow linear growth of $V(N_2)$ at longer illumination times and at a rate characteristic of N_2O/ZnO^*. As already noted, measurements of noncondensable product formation over uv illuminated $(CH_3)_3COH/ZnO^*$ interfaces were complicated by photoassisted growth of methane product. However, this complication did not arise with isopropanol and data to the right of the arrows in Fig. 3B for mixtures of N_2O with isopropanol over the illuminated ZnO surface confirm the contribution by an initial fast photoassisted process involving preadsorbed alcohol and nitrous oxide. It appeared from these results that this photoeffect could either represent a *direct* enhancement of Reactions (2a) and (2b) by illumination or an *indirect* enhancement of Reaction (1) due to hole trapping by alcohol.

The lack of any significant photoassisted dissociation to N_2 at the N_2O/TiO_2^* interface (cf. Fig. 4) argued against significant photocatalysis of Reaction (1) at that interface. Consequently no photoassisted formation of additional $O^-_{(ads)}$ intermediates from N_2O was thought to occur at N_2O/TiO_2^* interfaces. Plots 4A (ii) and 4B (ii) demonstrate, however, that readily measurable rates of N_2 production were observed when ethanol or isopropanol was simultaneously present with N_2O at the illuminated TiO_2 surface. One working hypothesis capable of explaining these observations was that illumination of the TiO_2 surface directly produced surface $O_{(ads)}^-$ intermediates without the need to photodissociate N_2O (e.g., by trapping photogenerated holes at preexisting coordinatively unsaturated O^{2-} ions). Reaction of adsorbed alcohol with such O^- entities via Reaction (2a) to produce secondary surface radicals capable of reacting with N_2O via Reaction (2b) would then account for the additional N_2 observed on illumination—despite the absence of O^- fragments from N_2O photodissociation. In the context of the hypothesis that lattice $O^=$ species act as a *direct* hole trap, the absence of any photoassisted nitrogen product formation over TiO_2 or ZnO in the presence

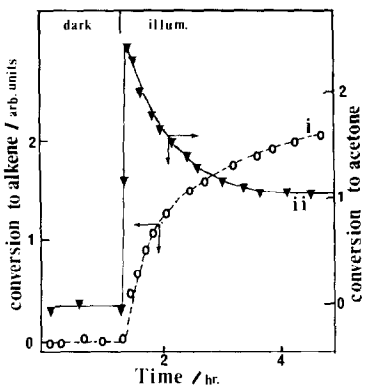

FIG. 7. Data obtained with the dynamic flow photoreactor showing growth of dynamic partial pressure of gaseous photoproducts over a $(CH_3)_3COH/ZnO$ interface at room temperature under continuous illumination by photons of $\lambda = 340$–640 nm at alcohol pressure of 3×10^{-4} N m^{-2}. The single vertical line denotes start of illumination. (i) Growth of dehydration product, 2-methylpropene (—○—); (ii) growth of acetone product, implying α–β bond rupture (—▼—).

of 2-methyl-propan-2-ol may be understood on the basis of reported low reactivity of O^- toward this tertiary alcohol [recall that the photoassisted increase in noncondensable products from $(CH_3)_3COH/ZnO^*$ shown in Fig. 3B plot (i) was due to formation of methane and not N_2]. An alternative hypothesis was that the initial fast photoassisted growth in nitrogen product resulted from an enhancement of dissociative electron attachment to adsorbed N_2O, made possible by adsorbed alcohol acting as an *indirect* hole trap, e.g., by electron tunnelling from adsorbed alcohol to a hole in the valence band. This hypothesis appeared less consistent with the observed failure of 2-methyl-propan-2-ol to promote photodissociation of N_2O, since tertiary alcohol should most readily lose an electron in an irreversible manner, due to greatest stability of the resultant tertiary cation.

B.4. Photoassisted Reactions in Dynamic Flow Conditions

Possibilities for loss of products from the gas phase by their readsorption onto the metal oxide surface represented an evident disadvantage of the static reactor results and prompted experiments with the dynamic flow photoreactor shown diagrammatically in Fig. 1B. Oxide samples were therefore prepared and pretreated as described in Refs. 35 and 36 and exposed to low dynamic pressures of reactant gas(es) at ca. 10^{-4} N m^{-2}, which were established over the samples as a balance between inlet leak rate of reactants through a metal variable leak valve and their removal by a continuously operating ion pump which gave an effective pumping speed of 1 liter sec^{-1} at the sample position. The large mean free path of molecules at 10^{-4} N m^{-2} should promote escape of desorbed species from the vicinity of the oxide surface and facilitate their entry into the ion-source region of the VG. Micromass 6 analyzer located 15 cm from the oxide surfaces along a high conductance path. The MM6 was employed for on-line gas analysis of reactant alcohols, or (alcohol + N_2O) mixtures in approximately 1:1 mole ratio, which were mass analyzed at various times prior to the commencement of illumination until reproducible reactant spectra were obtained. Continuous illumination of the GAS/SOLID interface was then commenced and the gaseous phase mass analyzed at various times during an illumination period of ca. 3 hr. Figure 7 illustrates the success of this technique in detecting directly the increases in partial pressures of dehydrated and demethanated species produced by the incidence of photons of $\lambda \sim 340$ to 640 nm upon a $(CH_3)_3COH/ZnO$ interface. Photons in this wavelength band were chosen to minimize any possibility of direct photolysis through light absorption by adsorbed alcohol or alkoxide (*37*).

The growth of 2-methyl-propene observed in these dynamic conditions agrees with the growth of this product detected for this system in the static photoreactor (cf. Fig. 6B). However, the initial burst

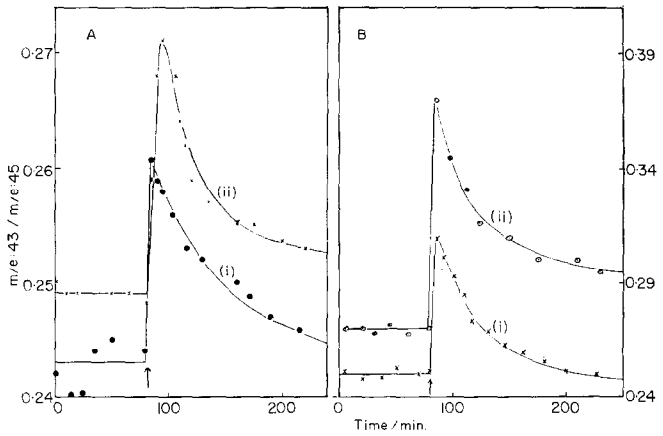

FIG. 8. Time profiles for appearance of increased dynamic partial pressures of dehydration and dehydrogenation products in the gas phase, as detected with Micromass 6 mass analyzer with isopropanol flowing over the metal-oxide catalyst at 3×10^{-4} N m^{-2}. Arrows denote the start of continuous illumination with photons at 254 nm. (Ai) Acetone from isopropanol/ZnO*; (Aii) acetone from N_2O + isopropanol/ZnO*. (Bi) Acetone from isopropanol/TiO_2*; (Bii) propene from isopropanol/TiO_2*.

of acetone photoproduct detected in the gas phase by the dynamic photoreactor technique was without parallel in the static photoreactor results and indicated the value of the dynamic method for direct detection of photoproducts which could become irreversibly adsorbed on the metal oxide in the static photoreactor.

The dynamic flow photoreactor was also utilized to examine the wavelength dependence and relative extents of photo-assisted dehydrogenation and dehydration for the secondary alcohols, isopropanol and butan-2-ol, and the primary alcohols, 2-methyl-propan-1-ol and ethanol. The wavelength dependence was examined by comparing results obtained for illumination of the interface by 4×10^{17} photons sec^{-1} mainly at 254 nm (but distributed 200–400 nm) with results obtained under illumination by 6×10^{17} photons sec^{-1} mainly at 365 nm (but distributed 300–1000 nm). Qualitatively similar results were observed with each type of illumination, an observation which made it appear improbable that the photoeffects arose from direct photolysis of preadsorbed alcohol, since photons at $\lambda > 300$ nm were unlikely to be absorbed by adsorbed alcohol. Typical results (obtained under illumination by photons mainly at 254 nm) are shown in Fig. 8 for isopropanol/metal-oxide interfaces. The lower curve of Fig. 8A illustrates photoassisted production of the dehydrogenation product, acetone, upon illumination of an *iso*propanol/*ZnO** interface through quartz. Note the rapid initial increase in gas phase acetone, reaching a maximum approximately 4 min after the commencement of uv illumination. This increase was followed by a slow decrease in dynamic pressure of acetone until, at times ~170 min after the commencement of illumination, photodehydrogenation had ceased. Data to the left of the arrow in the diagrams in Fig. 8 were obtained prior to the commencement of uv illumination and show that presence of (N_2O + isopropanol) in 1:1 mole ratio as the gas phase flowing over the "dark" ZnO interface resulted in a larger preillumination level of acetone formation (Fig. 8A, upper plot). Data to the right of the arrow in the upper plot show that the initial photoenhanced formation of acetone was larger and was sustained for longer times in the presence of N_2O.

TABLE 4

Extent of Photoassisted Dehydration ($-H_2O$), Dehydrogenation ($-H_2$), and α–β Bond Cleavage (α–β) at *Alcohol-Vapor/Metal-Oxide* Interfaces under Dynamic Conditions[a]

	ZnO*			TiO_2*		
Reactant gases	$(-H_2O)$[b]	$(-H_2)$[c]	$(\alpha$–$\beta)$[d]	$(-H_2O)$[b]	$(-H_2)$[c]	$(\alpha$–$\beta)$[d]
C_2H_5OH	—	5×10^{17}	—	—	2.2×10^{18}	—
$N_2O + C_2H_5OH$	—	1.4×10^{18}	—	—	4.6×10^{18}	—
$(CH_3)_2CHOH$	—	7.2×10^{17}	—	3.8×10^{17}	2.8×10^{18}	—
$N_2O + (CH_3)_2CHOH$	—	1.5×10^{16}	—	—	5.2×10^{18}	—
$(CH_3)_3COH$	2.2×10^{18}	—	1.6×10^{18}	3.6×10^{18}	—	3.6×10^{18}
$N_2O + (CH_3)_3COH$	1.7×10^{18}	—	2.9×10^{18}	1.2×10^{18}	—	6.8×10^{18}
$(CH_3)_2CHCH_2OH$	—	5.8×10^{17}	—	—	1.6×10^{18}	—
$CH_3CH_2CH(OH)CH_3$	2.0×10^{17}	8.6×10^{17}	—	3.0×10^{17}	2.6×10^{18}	—

[a] Values are normalized as molecules released per m^{-2} of oxide surface.
[b] Measured as alkene product—these are not limiting values.
[c] Measured as aldehyde or ketone dehydrogenated with respect to parent alcohol—these are limiting values.
[d] Evaluated from acetone product.

These observations are consistent with some production of additional O^- species from N_2O on the dark or illuminated ZnO interface and with reaction of these O^- species to yield dehydrogenated product via reactions of type (2a) and (2b). Data on the upper plot of Fig. 8A at times >60 min illumination indicate a small net increase in acetone, corresponding to a small continuing rate of photoassisted dehydrogenation in the photostationary state, presumably via Reactions (2a) and (2b). Nitrogen corresponding to this process was detected in the static photoreactions [cf. Fig. 2A (ii)].

Data in Fig. 8B illustrate the photoassisted growth of both the dehydration product, propene, and the dehydrogenation product, acetone, above a uv-illuminated isopropanol/TiO_2* interface. Comparison of Figs. 8A and B confirm the greater activity of the TiO_2 surface for these photoassisted elimination reactions involving isopropanol. Since a quantitative measure of the extent of each photoassisted elimination reaction was desirable, values for the total amount of gaseous photoproducts which desorbed from the illuminated interfaces over the observed time intervals were derived by graphically integrating the areas under plots of the form shown in Figs. 7 and 8 and applying the following equation developed by Becker (*38*) and Becker and Hartmann (*39*) for evaluating $(q_0 - q_t)$, the amount of gas desorbed in time t in flash-desorption experiments.

$$\text{Amount desorbed} = \frac{1}{AkT_0}\left[V\Delta P(t) + S\int_0^t \Delta p\, dt\right]. \quad (5)$$

In this equation, k is Boltzmann's constant, A = surface area of adsorbent, T_0 = gas temperature, V = volume of reaction system, S = pumping speed, and $\int_0^t \Delta p\, dt$ is the area under pressure-versus-time curves such as are shown in Figs. 7 and 8. Increases in peak height obtained experimentally for various mass numbers were converted to pressure changes Δp, and substituted into Eq. (5), thereby yielding values for the total number of molecules of each product desorbing in a given time interval (usually 0–170 min after the commencement by uv illumination). Those values are tabulated in Table 4 for the alcohol/metal-oxide systems studied. In relation to photodehydration, these data show that the extent of reaction of teritiary butanol was an order-of-magnitude greater than for secondary alcohols at the same interface, while primary alcohols did not experience photodehydration to measurable extent.

Extent of photodehydrogenation of primary or secondary alcohols (see columns headed "$-H_2$" in Table 4) did not show large variations with the identity of these alcohols. The tertiary alcohol represented an obvious exception to this behavior since dehydrogenation via an initial α-hydrogen abstraction was not possible. Results in Table 4 and Fig. 6 show that other photo-assisted process(es) yielding methane and acetone photoproducts replaced photo-dehydrogenation at 2-methyl propan-2-ol/metal-oxide* interfaces. These are denoted in Table 4 as photoassisted α–β bond cleavage.

DISCUSSION

The literature provided evidence that surfaces of ZnO samples outgassed *in vacuo* at 623–673 K for 16 hr were extensively dehydroxylated (*3*, *29*). A similar conclusion was previously arrived at by Bickley *et al.* (*7*a) in relation to rutile surfaces on the basis of their observations that surface hydroxyls enhanced oxygen photoadsorption and that activity of the specimen for photodesorption of oxygen could be completely destroyed by prolonged outgassing. This point was checked for the "prereduced" TiO_2 surfaces, i.e., outgassed for 16 hr at 673 K in the present study, by admitting oxygen at room temperature and testing whether any photoadsorption was observable. Since none was found, it was concluded that the "prereduced" TiO_2 surfaces resembled the ZnO surfaces in being initially in an extensively dehydroxylated condition and that preexisting hydroxyl groups were unlikely to play an important role in the initial interactions of alcohols and/or nitrous oxide with the prereduced surfaces. This conclusion was strongly supported for the nonilluminated surfaces of ZnO and TiO_2 by our observation that the preadsorption of alcohol onto both these prereduced surfaces (which could be expected to increase the degree of surface hydroxylation) inhibited the activity of the surfaces for the "dark" dissociation of any N_2O subsequently admitted. That observation was in marked contrast to the enhancement of the extent of N_2O dissociation noted when the alcohol and N_2O were simultaneously admitted (cf. Figs. 3 and 4 and Table 2). As noted above, this enhancement can best be explained on the basis that N_2O dissociation by one-electron transfer at preexisting nonhydroxylated sites yielded O^- intermediates which then underwent reactions of type (2a) and (2b), thereby dehydrogenating the alcohol and causing further N_2O dissociation.

Results obtained previously (*4*) with ZnO and TiO_2 samples prereduced by procedures similar to those used in the present study allowed estimates of the surface concentration of one-electron-donor sites to be made as 10^{16} for ZnO and 5×10^{17} m^{-2} for TiO_2. Since the extents of dehydration here detected for alcohols adsorbed onto prereduced surfaces at 300 K greatly exceeded those surface concentrations of one-electron donors (usually by an order of magnitude—cf. Table 3), it may be concluded that other types of sites were active for alcohol dehydration at the nonilluminated surfaces. The sequence of dehydrating activity exhibited by TiO_2 toward various alcohols, viz. tertiary > secondary > primary, suggested an important role for surface features which confer Lewis acid–base character to the vacuum outgassed surfaces, e.g., coordinatively unsaturated $O_{cus}^{=}$ or Ti_{cus}^{4+} on TiO_2. These represented likely alternative active sites capable of existing at the surface concentration levels implied by data in Table 3 for dehydration at nonilluminated interfaces. Data in Table 3 for uv-illuminated interfaces show an illumination-induced enhancement in the amount of alkene product observed during subsequent thermal desorption which was particularly evident for alcohol/TiO_2* interfaces, although also observable for ZnO. The

results shown in Figs. 6B and 7, together with relevant data in Table 4, provide evidence that photodehydration was an important and continuing photoeffect for the tertiary alcohol over both TiO_2 and ZnO. Tests with isopropanol at prereduced TiO_2 or ZnO surfaces at 300 K in identical conditions to the experiment illustrated in Fig. 6 for 2-methyl-propan-2-ol yielded no detectable yield of alkene or alkane product in the gas phase. This marked difference in stability between the tertiary and secondary alcohol at the uv-illuminated metal oxide surface would be fully consistent with dependence of photodehydration upon formation of a cation radical from the alcohol by hole trapping. On the basis of the much greater stabilities reported for the cation radicals from tertiary alcohols, a much larger photostationary concentration of this cation could be expected to result from hole trapping at the $(CH_3)_3COH$/metal-oxide* interface than at interfaces involving secondary or primary alcohols. More favorable hole trapping by the tertiary alcohol may therefore be advanced as one factor contributing to the unique ability of 2-methyl-propan-2-ol to undergo continuing photodehydration. Another factor was undoubtedly the existence of an alternative channel for photooxidation for the primary and secondary alcohols, viz. photodehydrogenation.

A marked difference between the time profile for release of photodehydrogenated product and that just discussed for photodehydration can be seen by comparing traces in Fig. 8A with trace (i) of Fig. 7. Time profiles similar to those in Fig. 8A were also observed for acetaldehyde formation from ethanol/TiO_2* or ethanol/ZnO* and for the other primary and secondary alcohols in Table 4. The shape of these time profiles, with partial pressure of dehydrogenated product falling to insignificant levels after ca. 3 hr illumination of the interface under a dynamic pressure of 3×10^{-4} N m^{-2} of the reactant alcohol, pointed to an inherent limitation on photodehydrogenation at the prereduced ZnO or TiO_2 surface. Such limitations have been noted by previous workers in the absence of an oxidizing gas (*7*, *9*). The evidence developed in the present paper for the important role of surface O^- species in dehydrogenation makes it appear probable that O^- species generated from lattice O^{2-} ions at the surface, following localization of a photogenerated hole or exciton, would confer activity for the abstraction of an α-hydrogen from primary or secondary alcohol. Such photoactivity would be limited to values of the magnitude listed under columns headed "$-H_2$" in Table 4 if each lattice $O^=$ ion at the surface could promote just one dehydrogenation and thereafter be poisoned.

Histogram (i) in Fig. 5 indicates that the hydrogen product from dehydrogenation may not desorb at room temperature. Consequently it appears possible that the fall-off in activity for photodehydrogenation of isopropanol, which is evident in Fig. 8A, resulted from gradual poisoning of surface $O^=$ sites by retention of hydrogen photoproduct. Curve (ii) of Fig. 8B shows that activity of the same surface for the simultaneous production of propene declined with duration of illumination in a manner similar to that for acetone production, i.e., photodehydration fell off in parallel with photodehydrogenation for the secondary alcohol. This result would be consistent with dependence of both photoeffects upon the same primary light-indicated process, viz. hole trapping by surface $O^=$ sites, and with poisoning of the surface toward that primary process through retention of hydrogen product. No such poisoning would be expected in the presence of an adequate pressure of gases capable of oxidizing hydrogen on the surface in condition of the photocatalytic experiment, which would be consistent with the many previous reports

of continuing photodehydrogenation in the presence of molecular oxygen.

The mechanism proposed here for photodehydrogenation is essentially rather similar to that developed by other workers for oxygenated systems, but with the difference that lattice O_{cus}^{2-} are here represented as *directly* trapping photogenerated holes to yield a limited number of readily poisoned sites for dehydrogenation. Mechanisms developed previously for oxygenated systems (*7*, *9*, *40*, *41*) envisaged *direct* and repeated hole trapping at sites featuring surface hydroxyls and represented molecular oxygen as providing the complementary electron trapping essential for continuing photodehydrogenation. Our observation of a high initial rate of photodehydrogenation was not unexpected by analogy with these published mechanisms, since rate constants for abstraction of an α-hydrogen from an alcohol by O^- or OH in homogeneous systems (*19*, *42*, *43*) usually lie within a factor of two of each other, a similarity which, incidentally, makes it impossible to exclude the possibility of some contribution to photodehydrogenation in the present study by hole trapping at residual surface hydroxyls on the prereduced metal oxides. The failure of N_2O to promote continuing photodehydrogenation of isopropanol in a manner similar to molecular oxygen was unexpected in terms of an analogy with the oxygenated system, in view of the reported efficiency of N_2O as an electron trap. In terms of the mechanism proposed here for prereduced surfaces this difference between N_2O and oxygen would be explicable on the basis that N_2O failed to oxidize hydrogen product from photodehydrogenation.

Figures 6 and 7 show that continuing photodehydration of 2-methyl-propan-2-ol was initially accompanied by photoassisted formation of methane and acetone over either ZnO or TiO_2 surfaces but that efficiency of these photoeffects, which imply cleavage of an α–β carbon–carbon bond of the tertiary alcohol, decreased with duration of illumination, except in the case of methane from $(CH_3)_3COH/TiO_2$*. The mechanism and time dependence of photoassisted α–β bond cleavage of the tertiary alcohol are not yet understood but are being further studied to assess contributions by *direct* and *indirect* hole trapping.

ACKNOWLEDGMENTS

Maintenance grants to D. J. M. and E. L. G. from the Department of Education of the Irish Government are acknowledged with thanks, together with technical assistance by B. Doyle, J. Caffrey, and M. McBrearty.

REFERENCES

1. Cunningham, J., Kelly, J. J., and Penny, A. L., *J. Phys. Chem.* **74**, 1992 (1970).
2. Cunningham, J., Kelly, J. J., and Penny, A. L., *J. Phys. Chem.* **75**, 617 (1971).
3. Cunningham, J., and Penny, A. L., *J. Phys. Chem.* **76**, 2353 (1972).
4. Cunninghan, J., and Penny, A. L., *J. Phys. Chem.* **78**, 870 (1974).
5. Morrison, S. R., and Freund, T., *Electrochem Acta* **13**, 1343 (1968).
6. Gomes, W. P., Freund, T., and Morrison, S. R., *J. Electrochem. Soc.* **115**, 818 (1968).
7. (a) Bickley, R. I., Munuera, G., and Stone, F. S., *J. Catal.* **31**, 398 (1973); (b) Bickley, R. I., and Stone, F. S., *J. Catal.* **31**, 389 (1973).
8. Bickley, R. I., and Jayanty, R. K. M., *Discuss. Faraday Soc.* **58**, 194 (1974).
9. Cundall, R. B., Rudham, R., and Salim, M. S., *J.C.S. Faraday I* **7**, 1642 (1976).
10. Goodenough, J. B., *Progr. Solid State Chem.* **5**, 344 (1971).
11. Chon, H., and Prater, C. D., *Discuss. Faraday Soc.* **41**, 380 (1966).
12. Walker, A., Formenti, M., Meriaudeau, P., and Teichner, S. J., *J. Catal.* **50**, 237 (1977).
13. Cunningham, J., Hodnett, B. K., and Walker, A., *Proc. Roy. Irish Acad. RIC Centenary Issue* **77 B**, 411 (1977).
14. Marx, R., Mauclaire, G., Feshenfield, F. C., Dunkin, D. B., and Ferguson, E. E., *J. Chem. Phys.* **58**, 3267 (1973).
15. Anbar, M., and Neta, P., *Int. J. Appl. Rad. Isotopes* **18**, 493 (1967).
16. Lunsford, J. H., Taarit, Y. B., and Wong, N. B., *J. Chem. Phys.* **60**, 2148 (1974).
17. Warman, J. M., *J. Phys. Chem.* **72**, 52 (1968).

18. Warman, J. M., *Nature (London)* **213**, 381 (1967).
19. Neta, P., and Schuler, H., *J. Phys. Chem.* **79**, 1 (1975).
20. Che, M., Naccache, C., and Imelik, B., *J. Catal.* **24**, 328 (1972).
21. Hosaka, H., Fujiwara, T., and Meguro, K., *Bull. Chem. Soc. Japan* **44**, 2616 (1971).
22. Pimenov, Y. D., Kholmogorov, V. E., and Terenin, A. N., *Doklady Akad. Nauk SSSR* **163**, 935 (1965).
23. (a) Ueda, H., *Bull. Chem. Soc. Japan* **43**, 319 (1970); (b) Kiselev, A. V., and Uvarov, A. V., *Surface Sci.* **6**, 399 (1967).
24. Davison, R. S., and Slater, R. M., *J.C.S. Faraday Trans. I*, **72**, 2416 (1976).
25. (a) Knözinger, H., Krietenbrink, H., Muller, H. D., and Schulz, W., "Proceedings of the Sixth International Congress on Catalysis" (London, 1976), p. 183. Chem. Soc. (London), 1977; (b) Thomke, K., "Proceedings of the Sixth International Congress on Catalysis" (London, 1976), p. 303. Chem. Soc. (London), 1977.
26. Zanderighi, L., Greco, A., and Carrà, S., *J. Catal.* **33**, 327 (1974).
27. Figueras, F., Nohl, A., Mourges, L., and Trambouze, Y., *Trans. Faraday Soc.* **67**, 1155 (1971).
28. Tret'yakov, N. E., and Filimonov, V. N., *Kinet. Katal.* **13**, 735 (1972) (trans.).
29. Atherton, K., Hockey, J. A., and Newbold, G., *Discuss. Faraday Soc.* **52**, 33 (1971).
30. Perry, E., *J. Catal.* **2**, 371 (1963).
31. Banthorpe, B. V., "Elimination Reactions." Elsevier, London, 1963.
32. Pines, H., and Manassen, J., *Advan. Catal.* **16**, 49 (1966).
33. McArthur, D. P., Bliss, H., and Butt, J. B., *J. Catal.* **28**, 183 (1973).
34. Cunningham, J., and Meriaudeau, P., *J.C.S. Faraday Trans. I* **72**, 149 (1976).
35. Cunningham, J., and Samman, N., *in* "Dynamic Mass Spectrometry" (D. Price and J. Todd, Eds.), Vol. 4, p. 247. Heyden & Sons, London, 1976.
36. Cunningham, J., Finn, E., and Samman, N., *Discuss. Faraday Soc.* **58**, 160 (1974).
37. Kubota, S., Iwaizumi, M., and Isobe, T., *J. Phys. Chem.* **77**, 2837 (1973).
38. Becker, J. A., *Advan. Catal. 7*, 135 (1955).
39. Becker, J. A., and Hartmann, C. D., *J. Phys. Chem.* **57**, 157 (1953).
40. Boonstra, A. H., and Mutsaers, C. A. H. A., *J. Phys. Chem.* **75**, 1694 (1975).
41. Guelton, M., Ridge, M., Bonnelle, J. P., and Beaufils, J. P., *J. Chim. Phys.* **72**, 1279 (1975).
42. Czapski, G., Sammuni, A., and Meisel, D., *J. Phys. Chem.* **75**, 3271 (1971).
43. (a) Sicilio, F., and Lewis, E. L., *J. Phys. Chem.* **73**, 2590 (1968); (b) Sicilio, F., and James, R. S., *J. Phys. Chem.* **74**, 1166 (1970)